Check for updates

2022 early-summer heatwave in Southern South America: 60 times more likely due to climate change

Juan Antonio Rivera[1] [ORCID] · Paola A. Arias[2] · Anna A. Sörensson[3,4,5] · Mariam Zachariah[6] · Clair Barnes[6] · Sjoukje Philip[7] · Sarah Kew[7] · Robert Vautard[8] · Gerbrand Koren[9] · Izidine Pinto[7] · Maja Vahlberg[10] · Roop Singh[10] · Emmanuel Raju[11] · Sihan Li[12] · Wenchang Yang[13] · Gabriel A. Vecchi[13,14] · Luke J. Harrington[15] · Friederike E. L. Otto[6]

Abstract

A large area including the central-northern part of Argentina, southern Bolivia, central Chile, and most of Paraguay and Uruguay, experienced record-breaking temperatures during two consecutive heatwaves in late November and early December 2022. During the second heatwave, nine locations in northern Argentina registered their highest maximum temperature of December since at least 1961. Our analysis based on observational and reanalysis datasets indicate that South America, like the rest of the world, has experienced heatwaves increasingly frequently in recent years. The December 2022 heatwave has an estimated return time of 1 in 20 years in the current climate, meaning it has about a 5% chance of happening each year. To estimate how human-caused climate change has influenced the likelihood and intensity of the observed heatwave, we combined climate models with the observation-based data. We found that human-caused climate change made the event about 60 times more likely. A heatwave with a return period of 20 years would be about 1.4 °C less hot in a world without anthropogenic global warming. Heatwaves this early in the summer season pose a substantial risk to human health and are potentially lethal. This risk is aggravated by climate change, but also by other factors such as an aging population, urbanisation and the built environment, and individual behavior and susceptibility to the heat. This highlights the importance of attribution studies in a region already threatened and vulnerable to climate change.

Keywords Southern South America · Heatwave · Attribution · Impacts · Vulnerability

1 Introduction

The Sixth Assessment Report (AR6) of the Intergovernmental Panel on Climate Change (IPCC) assesses that it is virtually certain that the duration, frequency and intensity of hot extreme events at global scale, such as heatwaves, are increasing due to human activity (IPCC 2021; Seneviratne et al. 2021). Over most of South America, an increase in the intensity and frequency of heatwave events since 1960 has been detected (Ceccherini et al.

2016; Rusticucci et al. 2016; Geirinhas et al. 2018), with high confidence in the attribution to human activity in South-Eastern South America and medium confidence in South-Western South America (Seneviratne et al. 2021). In Argentina, even when the mean warming is below the global average, a marked increase in the occurrence and duration of heatwaves has been observed (Barros et al. 2015; Rusticucci et al. 2016). The heatwave that affected northern and central Argentina in December 2013 was exacerbated by anthropogenic forcings, with best-guess estimates of the event probability increasing by a factor of five (Hannart et al. 2015; Otto et al. 2017). Often, heatwaves tend to occur simultaneously with droughts, creating a compound climate event that can have enormous impacts at regional level. Under ongoing anthropogenic climate change, there is a complex interaction between increased precipitation and increased temperatures for Southeastern South America (van Garderen and Mindlin 2022).

IPCC (2021) assessed that it is very likely that the intensity and frequency of hot extremes such as the days with maximum temperature above 35 °C or the annual hottest daily maximum temperature (TXx) will continue increasing in South America, compared with the 1995–2014 baseline, even under 1.5 °C global warming (see for example Table 11.13 of Seneviratne et al. 2021; and Table 12.6 of Ranasinghe et al. 2021). This is also evident over South-Eastern South America, where the observed trend in frequency and intensity of heatwaves is expected to increase even for moderate warming scenarios as the RCP4.5 (Feron et al. 2019). Significant changes in several climate indicators related to temperature extremes are also projected over the region, with increases in the frequency of warm nights and days and decreases in the indices related to cold extremes (Cabré and Nuñez 2020; Feron et al. 2019; Reboita et al. 2022).

Since late austral spring, several regions of Southern South America experienced the occurrence of heatwaves, in a warm season that was record breaking in terms of frequency over Argentina according to its National Weather Service (SMN) (SMN 2023). An area comprising the central-north part of Argentina, southern Bolivia, central Chile, and most of Paraguay and Uruguay, experienced record-breaking temperatures as a consequence of two consecutive heatwaves since mid-November. From 23 to 29 of November, a heatwave (defined as the period with at least three consecutive days with maximum and minimum temperatures above the 90th percentile, Rusticucci et al. 2016) was declared by the SMN for 19 stations located in the latitudinal band from 28° to 37°S (SMN 2022a). During this period, temperature anomalies exceeded 5 °C over this region and some stations recorded maximum temperatures of more than 40 °C. Over Uruguay, the National Institute of Meteorology (INUMET) reported that most stations recorded temperatures above the upper tercile during the last part of November (INUMET 2022a). A larger area, extending far south towards Patagonia, showed record-breaking temperatures for November, with 14 locations setting new maximum temperature records. It is noteworthy that these record temperatures occurred before the beginning of the austral summer season, making them particularly exceptional. Moreover, these events happened just a few days after record-breaking cold conditions took place over central Argentina and Uruguay (SMN 2022b).

A second period of prolonged hot weather was recorded during the first quarter of December 2022, just a few days after the November heatwave. The highest severity was observed in the same latitudinal band of the previous event, although the spatial extension covered roughly half of Argentina, with heatwave durations ranging between 3 and 9 days. According to the SMN (2022c), 45 stations recorded heatwave conditions between 4 to 12 of December. Among these stations, maximum temperatures above 40 °C were observed in 24 locations, with four of them exceeding 45 °C. For instance, Rivadavia station, located near the border with Bolivia and Paraguay, recorded 46 °C of maximum temperature

during December 7, making the region one of the hottest in the World during that day. Averaged over the first 10 days of December, temperature anomalies were above + 4 °C north of 40°S, with some specific locations exceeding + 10 °C above normal conditions, particularly between 7 to 9 of December. During this period, 9 locations from northern Argentina registered their highest maximum temperature of December since at least 1961. A special bulletin for persistent high temperatures was issued by the Directorate of Meteorology and Hydrology of Paraguay (DMH) on December 7, with the probability of experiencing a heatwave over much of Paraguay (DMH 2022). For instance, western Paraguay registered maximum temperatures above 40 °C between 6 to 9 of December, equaling the all-time record at Mariscal Estigarribia during December 8. At the same time, the Uruguayan Institute of Meteorology released a heatwave warning, particularly for the western portion of Uruguay (INUMET 2022b).

The two consecutive heatwaves occurred during the multi-year drought that started in 2019. This large-scale drought started due to precipitation deficits and has worsened over time (Naumann et al. 2023), likely partly due to the continuing La Niña conditions that tend to have a drying effect on the region (Cai et al. 2020). Typically, heatwaves are linked to a persistent atmospheric blocking that favors the presence of warm air masses for several consecutive days over South-Eastern and South-Western South America. This can contribute to high temperature anomalies which might be reinforced if the regions are affected by drought conditions due to extremely low soil moisture (Alvarez et al. 2019; Marengo et al. 2022). The persistence of an anticyclonic circulation at various levels of the troposphere favors subsidence conditions and intense solar heating, intensifying the warming process, which might also be reinforced by horizontal temperature advection and an intensification of the South Atlantic Convergence Zone (SACZ) (Campetella and Rusticucci 1998; Cerne et al. 2007; Alvarez et al. 2019).

This study aims to identify to which extent human-induced climate change altered the frequency of occurrence of the heatwave observed in Southern South America during December 2022. To do this we use different observational and reanalysis datasets as well as simulations from different global and regional models. Section 2 describes the data and methodology used. Section 3 discusses the main findings from observational and reanalysis data. Section 4 performs an evaluation of the different models used in our study, presents the results from the heatwave event attribution using different methodologies and models and summarizes the main hazards associated with the heatwave. Section 5 discusses the main aspects of vulnerability, exposure and impacts during the heatwave. Finally, Sect. 6 presents a summary and discussion.
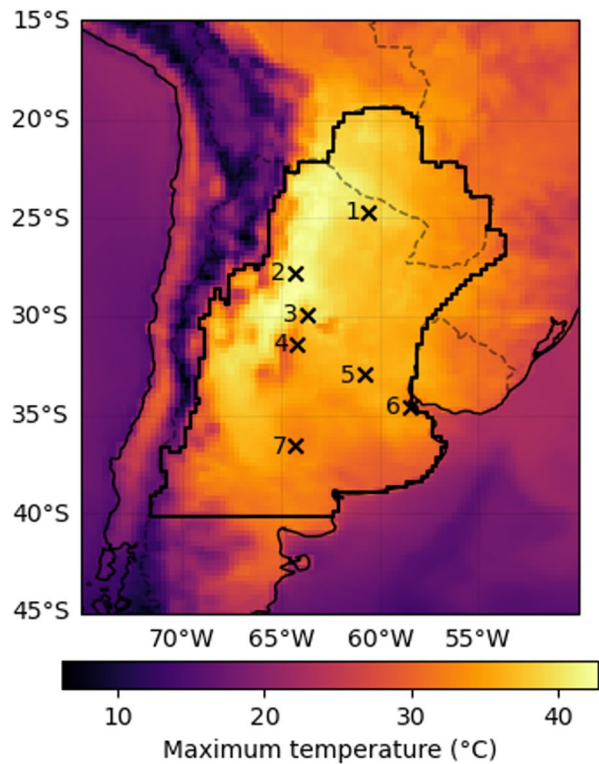
2 Data and methods

2.1 Observational data

To investigate the extent to which human-caused climate change altered the frequency of occurrence of the extremely high temperatures, we choose to analyse the 2-m temperature over land in the region covering northern Argentina (north of 40°S) and Paraguay, excluding high altitudes (highlighted by black outline in Fig. 1). This region includes the areas under red alert from the Argentinian Weather Service and includes the cities with the highest impacts. To account for the event itself, which lasted for about a week with durations at different locations ranging from 3–9 days, we decided to analyse the annual

Fig. 1 7-day average daily maximum temperature (TX7x) for the period of the 4th to 10th of December 2022 from ERA5 data. The bold black outline represents the study region and the crosses mark stations used in the observational analysis: 1. Las Lomitas; 2. Santiago del Estero; 3. Villa María del Río Seco; 4. Córdoba; 5. Rosario; 6. Buenos Aires; 7. Santa Rosa

(July-June) maximum of the 7-day average of daily maximum temperatures (TX7x) over this region. Figure 1 shows the 2022 event that occurred during 4–10 December. Additionally, we analyse the change in frequency and intensity of the maximum observed 7-daily temperature of 2022 at 7 locations, indicated as crosses in Fig. 1. These include the cities of Buenos Aires, Córdoba and Rosario. Even when some parts of southern Bolivia or western Uruguay show high temperatures during the analysed period (Fig. 1), its inclusion is not expected to result in a significant change in the results given that the areas would be limited in comparison with the whole central and northern Argentina and Paraguay.

We use the European Centre for Medium-Range Weather Forecasts (ECWMF) ERA5 reanalysis data (Hersbach et al. 2020). The reanalysis that runs up to the end of November 2022 is supplemented with analysis data up to 11 December. The second dataset is the gridded dataset of daily temperature known as the Climate Prediction Center (CPC) Global Unified Daily Gridded Temperature data, that is provided by the NOAA PSL through their website (https://psl.noaa.gov/). This data is available at $0.5° \times 0.5°$ resolution, for the period 1979-present. Maximum temperatures from both datasets are used for analysing the heatwave event in question in the context of climate change. As a measure of anthropogenic climate change, we use the (low-pass filtered) global mean

surface temperature (GMST). GMST is taken from the National Aeronautics and Space Administration (NASA) Goddard Institute for Space Science (GISS) surface temperature analysis (GISTEMP; Hansen et al. 2010; Lenssen et al. 2019).

Time series of daily maximum and minimum temperatures from January 1961 to December 12th 2022 at the locations shown in Fig. 1 were used to evaluate the ERA5 reanalysis and to evaluate local trends in return times. These station data were provided by the SMN. The selected stations cover the three largest cities in Argentina (Buenos Aires, Córdoba and Rosario), with three sites in the hottest part of the December heatwave, and one (Santa Rosa) in the cooler southern region.

2.2 Model and experiment descriptions

We used several model ensembles with different characteristics such as resolution, coupling and processes as follows:

2.2.1 CMIP6

We used simulations from general circulation models included in the sixth phase of the Coupled Model Intercomparison Project (CMIP6) (Eyring et al. 2016). We used all simulations of the daily maximum temperature available at the Institut Pierre-Simon Laplace (IPSL) Earth System Grid Federation (ESGF) node from their first realization (denoted r1iXpYfZ), where X, Y and Z can vary (but we select only one of each), without considering ensembles, as they have a very heterogeneous number of members. This led to the selection of 28 simulations from different coupled models. The resolution varies depending on the model but stays above 50 km. All temperatures are projected onto a $0.25° \times 0.25°$ grid before being spatially averaged over the study region (see Fig. 1).

2.2.2 CORDEX

We used all the COordinated Regional climate Downscalling EXperiment (CORDEX) simulations available at the IPSL ESGF node, separating them into two ensembles: CORDEX SAM-44 (14 different models with 0.44° resolution, i.e. about 50 km; Falco et al. 2019) and CORDEX SAM-22 (6 different models with resolution of 0.22°, about 25 km). CORDEX simulations result from a dynamical downscaling, using a regional climate model, of a general circulation model. As for CMIP6 simulations, temperatures are projected onto a $0.25° \times 0.25°$ grid (Gutowski et al. 2016) before being spatially averaged over the study region.

2.2.3 HighResMIP

This is a sea surface temperature (SST)-forced model ensemble (Haarsma et al. 2016), with simulations for the 1950–2050 period. The SST and sea ice forcings for the period 1950–2014 are obtained from the $0.25° \times 0.25°$ Hadley Centre Global Sea Ice and Sea Surface Temperature dataset that have undergone area-weighted regridding to match the climate model resolution (see Table 1). For the 'future' time period (2015–2050), SST/sea-ice data are derived from RCP8.5 (CMIP5) data, and combined with greenhouse gas forcings from SSP5-8.5 (CMIP6) simulations (see Sect. 3.3 of Haarsma et al. 2016 for further details).

Table 1 7-day maximum temperature in the year 2022, and the best estimates for return period, probability ratio and intensity change at seven individual stations in the study region

Station		Event magnitude [°C]	Return period [years]	Probability ratio (PR)	Intensity change (I) [°C]
No	Name				
1	Las Lomitas	43.014	40.4380	$> 1 \times 10^6$	1.804
2	Santiago del Estero	42.257	15.1540	3.8982	1.385
3	Villa María del Río Seco	39.986	15.6070	1.6568	0.686
4	Córdoba	39.100	17.2010	2.3102	0.984
5	Rosario	36.814	8.7029	7.4739	1.566
6	Buenos Aires	34.986	3.9540	9.5516	1.695
7	Santa Rosa	35.629	1.6589	2.3926	1.742

2.2.4 FLOR and AM2.5C360 models

The FLOR (Vecchi et al. 2014) and AM2.5C360 (Yang et al. 2021; Chan et al. 2021) climate models are developed at Geophysical Fluid Dynamics Laboratory (GFDL). The FLOR model is an atmosphere–ocean coupled GCM with a resolution of 50 km for land and atmosphere and 1 degree for ocean and ice. Ten ensemble simulations from FLOR are analysed, which cover the period from 1860 to 2100 and include both the historical and RCP4.5 experiments driven by transient radiative forcings from CMIP5 (Taylor et al. 2012). The AM2.5C360 is an atmospheric GCM based on that in the FLOR model (Delworth et al. 2012; Vecchi et al. 2014) with a horizontal resolution of 25 km. Three ensemble simulations of the Atmospheric Model Intercomparison Project (AMIP) experiment (1871–2050) are analysed. These simulations are initialised from three different pre-industrial conditions but forced by the same SSTs from HadISST1 (Rayner et al. 2003) after groupwise adjustments (Chan et al. 2021) over 1871–2020. SSTs between 2021 and 2050 are using the FLOR RCP4.5 experiment 10-ensemble mean values after bias correction. Radiative forcings are using historical values over 1871–2014 and RCP4.5 values after that.

2.2.5 UKCP18 land-GCM

This is a fifteen-member perturbed physics ensemble developed by the UK Met Office (Lowe et al. 2018). The ensemble members are derived from HadGEM3-GC3.05, a high-resolution coupled ocean–atmosphere model with horizontal grid spacing of approximately 60 km at mid-latitudes, which includes an explicit representation of atmospheric aerosols.

2.3 Statistical methods

In this study, we analyse time series from the region in the north of Argentina and Paraguay for July-June annual maxima of daily maximum temperature values (TX7x), where long records of observed data are available. Methods for observational and model analysis

and for model evaluation and synthesis are used according to the World Weather Attribution Protocol (Philip et al. 2020; Ciavarella et al. 2021; van Oldenborgh et al. 2021).

The analysis steps include: (i) trend calculation from observations; (ii) model evaluation; (iii) multi-method multi-model attribution and (iv) synthesis of the attribution statement. We calculate the return periods, Probability Ratio (PR; the factor-change in the event's probability) and change in intensity of the event under study in order to compare the climate of now and a counterfactual climate or climate of the past, defined respectively by the GMST values of now and of the preindustrial past (1850–1900, based on the Global Warming Index; https://www.globalwarmingindex.org). To statistically model the event under study, we use a Generalised Extreme Value (GEV) and GMST as a covariate. Next, results from observations and models that pass the evaluation tests are synthesized into a single attribution statement.

3 Observational analysis: return period and trend

3.1 Analysis of point station data

Figure 2 shows the time series of the annual maxima of 7-day average daily maxima for the seven selected stations: Las Lomitas, Santiago del Estero, Villa María del Río Seco, Córdoba, Rosario, Buenos Aires and Santa Rosa. We use this data for evaluating the performance of the gridded reanalysis products that are considered for this study. To do this, the station-based time series are overlaid with the values for the corresponding closest cell in the ERA5 reanalysis dataset, and the ERA5 regional mean. The station observations and the reanalysis-based values are found to be in good agreement for all stations (correlation > 0.7; statistically significant), providing confidence to the choice of ERA5 for capturing the event.

For each of these stations that are situated inside the study region, we also estimate the return period, the PRs and the intensity changes, as shown in Table 1. The 7-day maximum temperatures as high as those observed this year have return times ranging from 4 to 40 years, but the heat is rarer towards the northwest of the region. The 2022 event in Las
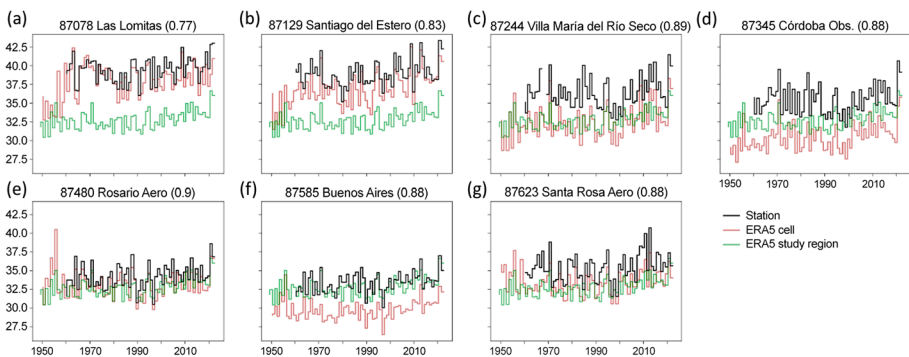

Fig. 2 7-day annual (July-June) maximum temperature at (**a**) Las Lomitas, (**b**) Santiago del Estero, (**c**) Villa María del Río Seco, (**d**) Córdoba, (**e**) Rosario, (**f**) Buenos Aires and (**g**) Santa Rosa, for the period 1961–2022. The red and the green lines show the corresponding estimates from the closest cell and the average over the study region, from the ERA5 reanalysis dataset, available for the years 1950–2022

Lomitas (Station 1 in Fig. 1) that incidentally records the highest temperature among these stations, would have been unlikely in a world without climate change (PR > 100).

3.2 Analysis of gridded data

Figure 3a shows the time-series of annual 7-day maximum of daily maximum temperature for the study region based on the two observed datasets- ERA5 (Fig. 3a) and CPC (Fig. 3b). There is an increasing trend in particular for the period 1979–2022 that is common to both datasets.

The left panels in Fig. 4 show the response of the study area-averaged annual 7-day maximum temperature based on ERA5 (Fig. 4(a left panel)) and CPC (Fig. 4(b left panel)) to observed GMST anomalies. The right panels (Fig. 4a and b) show the return period curves for the current, 2022 climate and a past climate that would have been 1.2 °C cooler as compared to now, based on the respective datasets. Using ERA5 data, the 2022 event is estimated to have a return period of 1-in-20 years in the current climate. However, the CPC dataset indicates that the same event has a return period of 1-in-10 years. The PRs suggest the tendency of such events becoming hotter and more
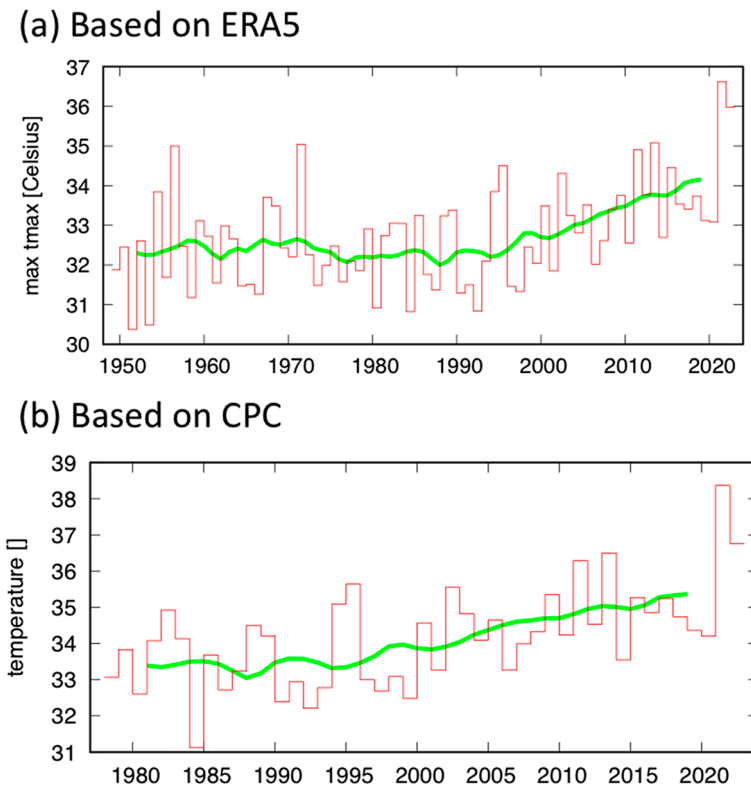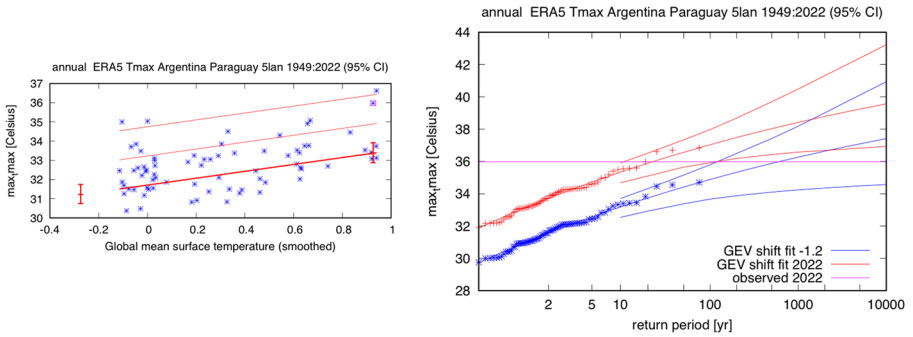

Fig. 3 Time series of annual 7-day maximum temperature, area-averaged over the study domain along with the 10 year running mean (shown by green line) based on (**a**) ERA5 and (**b**) CPC datasets
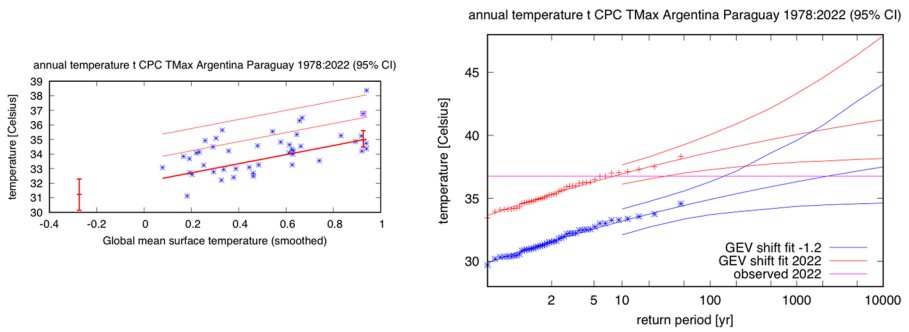
Fig. 4 a Left panel: Response of annual maxima of 7-day maximum temperature, averaged over the study region to change in global mean temperature, based on the ERA5 dataset. The thick red line denotes the time-varying mean, and the thin red lines show 1 standard deviation (s.d) and 2 s.d above. The vertical red lines show the 95% confidence interval for the location parameter, for the current, 2022 climate and the hypothetical, 1.2 °C cooler climate. The 2022 observation is highlighted with the magenta box. Right panel: GEV-based return periods for the 2022 climate (red lines) and the 1.2 °C cooler climate (blue lines with 95% Confidence Interval), based on the ERA5 dataset. **b** Same as **a**, based on the CPC dataset

frequent due to climate change. The PR is 26 [6-inf] based on ERA5 and 280 [13-inf] from CPC data, with intensity changes of 2.15 °C [1.3–3] and 3.75 °C [2.2–5.3], respectively.

Although there is a general agreement between the two datasets in their annual variability (Fig. 2) and their fits (Table S1 of the Supplementary Information), the CPC dataset is shorter (beginning in the year 1979), as opposed to ERA5 beginning in 1950. A careful examination of the trends in Fig. 4 also reveal a higher trend since 1980 in the ERA5 data that may have partially influenced this difference in the return periods, PR and intensity changes. Therefore, we select the longer ERA5 as the primary dataset for the event definition and for model evaluation. The return period used for model analysis for the annual 7-day maximum temperature is 20 years.

4 Model evaluation and multi-method multi-model attribution

4.1 Model evaluation

In this subsection we show the results of the model evaluation for the study region (Table S1). Per framing or model setup, we use models that only just pass the evaluation tests, if we only have five models or less for that framing that performs well. The climate models are evaluated against the observations in their ability to capture the seasonal cycle, the spatial pattern of the climatology, and the parameters of the fitted GEV model. The models are labeled as 'good','reasonable', or'bad', following the criteria defined in

Table 2 Probability ratio and change in intensity for models that passed the evaluation tests for (a) past vs. present (blue highlight) and (b) present vs. future (red highlight)

Observations/Model	a. Past vs. present		b. Present vs. future	
	Probability ratio PR [-]	Change in intensity ΔI [°C]	Probability ratio PR [-]	Change in intensity ΔI [°C]
ERA5	27 (5.7 ... ∞)	2.2 (1.3 ... 3.0)		
CPC	2.8e+2 (13 ... ∞)	3.7 (2.2 ... 5.3)		
	(...)	(...)		
CORDEX44-CNRMr1-RCA ()	13 (2.2 ... 1.0e+4)	0.87 (0.19 ... 1.6)	5.6 (0.00010 ... 31)	0.80 (0.30 ... 1.4)
CORDEX44-MK3r1-RCA ()	13 (2.1 ... 1.0e+4)	1.3 (0.36 ... 2.4)	5.5 (0.78 ... 41)	1.3 (0.41 ... 2.1)
CORDEX44-IPSLr1-RCA ()	4.0e+6 (19 ... 1.0e+4)	1.8 (1.1 ... 2.6)	7.0 (2.6 ... 98)	1.3 (0.81 ... 1.7)
CORDEX44-CORDEX44-MIROCr1-RCA ()	4.0 (0.95 ... 1.0e+4)	0.62 (-0.050 ... 1.3)	6.4 (0.00010 ... 36)	1.3 (0.45 ... 2.1)
CORDEX44-HADGEMr1-RCA ()	55 (2.2 ... 1.0e+4)	0.79 (-0.010 ... 1.4)	8.0 (3.1 ... 24)	1.3 (0.88 ... 1.7)
CORDEX44-MPIr1-REMO ()	23 (2.9 ... 1.0e+4)	1.6 (0.89 ... 2.2)	2.8 (1.1 ... 8.4)	0.72 (0.060 ... 1.3)
CORDEX44-MPIr1-RCA ()	19 (4.0 ... 1.0e+4)	1.6 (1.1 ... 2.1)	6.8 (3.2 ... 24)	1.3 (0.85 ... 1.8)
CORDEX44-NORESMr1-RCA ()	10 (1.3 ... 1.0e+4)	1.0 (0.17 ... 2.2)	5.0 (1.2 ... 36)	1.2 (0.49 ... 1.9)
CORDEX44-GFDLr1-	2.6 (0.060 ...	0.39 (-1.0 ... 1.7)	2.1 (0.58 ... 13)	0.47 (-0.18 ...

Table 2 (continued)

REGCM ()	1.0e+4)			1.1)
CORDEX44-GFDLr1-RCA ()	1.0e+4 (6.9 ... 1.0e+4)	1.2 (0.46 ... 2.0)	4.5 (0.00010 ... 2.2e+2)	0.99 (0.36 ... 1.6)
HighResMIP-HadGEM3-GC31-HM (1)	28 (5.3 ... ∞)	1.8 (1.0 ... 2.6)	(...)	(...)
HighResMIP-HadGEM3-GC31-LM (1)	4.1 (1.2 ... ∞)	0.90 (0.13 ... 1.9)	(...)	(...)
HighResMIP-HadGEM3-GC31-MM (1)	99 (7.7 ... ∞)	2.1 (1.3 ... 3.0)	(...)	(...)
HighResMIP-MPI-ESM1-2-HR (1)	7.1 (1.8 ... 95)	1.3 (0.48 ... 2.2)	(...)	(...)
HighResMIP-MPI-ESM1-2-XR (1)	3.1 (0.38 ... ∞)	0.43 (-0.55 ... 1.2)	(...)	(...)
UKCP18 land-GCM PPE (1) rcp85 ppe ()	5.3e+4 (16 ... 1.0e+6)	1.4 (0.57 ... 2.1)	5.9 (3.6 ... 50)	0.84 (0.65 ... 1.0)
UKCP18 land-GCM PPE (4) rcp85 ppe ()	1.6e+2 (8.1 ... 1.0e+6)	1.6 (1.0 ... 2.2)	3.8 (2.9 ... 5.8)	1.1 (0.89 ... 1.3)
UKCP18 land-GCM PPE (5) rcp85 ppe ()	47 (3.4 ... 1.0e+6)	1.6 (0.89 ... 2.4)	3.8 (2.3 ... 8.1)	0.83 (0.65 ... 1.0)
UKCP18 land-GCM PPE (6) rcp85 ppe ()	8.2e+2 (13 ... 1.0e+6)	2.0 (1.5 ... 2.5)	9.0 (4.7 ... 36)	1.0 (0.91 ... 1.2)
UKCP18 land-GCM PPE (7) rcp85 ppe ()	7.9e+2 (24 ... 1.0e+6)	1.9 (1.3 ... 2.5)	5.6 (3.7 ... 32)	1.2 (1.0 ... 1.5)
UKCP18 land-GCM PPE (9) rcp85 ppe ()	9.2 (3.4 ... 2.0e+2)	1.6 (1.1 ... 2.1)	3.6 (2.5 ... 6.6)	1.0 (0.85 ... 1.2)
UKCP18 land-GCM PPE (10) rcp85 ppe ()	7.7e+4 (9.1 ... 1.0e+6)	1.4 (0.83 ... 2.1)	5.6 (4.1 ... 8.7)	1.1 (0.89 ... 1.2)
UKCP18 land-GCM PPE (11) rcp85 ppe ()	3.4e+2 (7.3 ... 1.0e+6)	2.1 (1.4 ... 2.9)	5.9 (3.5 ... 17)	1.1 (0.98 ... 1.3)
UKCP18 land-GCM PPE (12) rcp85 ppe ()	3.2e+2 (9.5 ... 1.0e+6)	1.8 (0.90 ... 2.7)	5.3 (3.5 ... 21)	0.97 (0.75 ... 1.2)
UKCP18 land-GCM PPE (13) rcp85 ppe ()	8.6 (2.3 ... 1.0e+6)	0.91 (0.22 ... 1.5)	3.0 (2.3 ... 4.6)	0.74 (0.57 ... 0.91)

Table 2 (continued)

UKCP18 land-GCM PPE (15) rcp85 ppe ()	2.3e+3 (4.3 ... 1.0e+6)	1.4 (0.76 ... 2.0)	5.5 (3.7 ... 11)	0.95 (0.80 ... 1.1)
CMIP6-ACCESS-CM2_r1i1p1f1 ()	2.6 (0.44 ... 1.0e+4)	0.54 (-0.40 ... 1.4)	7.1 (0.00010 ... 28)	1.1 (0.76 ... 1.6)
CMIP6-ACCESS-ESM1-5_r1i1p1f1 ()	16 (3.0 ... 1.0e+4)	1.0 (0.37 ... 1.7)	7.5 (0.00010 ... 1.2e+2)	0.95 (0.61 ... 1.4)
CMIP6-CanESM5_r1i1p1f1 ()	2.2e+2 (13 ... 1.0e+4)	1.7 (1.1 ... 2.2)	4.9 (0.00010 ... 1.1e+2)	1.1 (0.82 ... 1.3)
CMIP6-CMCC-ESM2_r1i1p1f1 ()	3.7 (0.82 ... 1.0e+4)	0.61 (-0.12 ... 1.4)	6.5 (0.00010 ... 55)	1.3 (0.59 ... 2.0)
CMIP6-CNRM-CM6-1-HR_r1i1p1f2 ()	37 (3.5 ... 1.0e+4)	1.7 (0.86 ... 2.6)	4.9 (2.6 ... 19)	1.0 (0.66 ... 1.3)
CMIP6-CNRM-CM6-1_r1i1p1f2 ()	2.7 (0.29 ... 1.0e+4)	0.41 (-0.45 ... 1.3)	2.7 (1.2 ... 11)	0.74 (0.26 ... 1.2)
CMIP6-CNRM-ESM2-1_r1i1p1f2 ()	5.9 (1.1 ... 1.0e+4)	0.65 (-0.020 ... 1.3)	6.8 (0.00010 ... 41)	1.4 (0.85 ... 2.2)
CMIP6-EC-Earth3-CC_r1i1p1f1 ()	85 (4.5 ... 1.0e+4)	1.3 (0.59 ... 2.5)	2.5 (0.39 ... 14)	0.74 (-0.59 ... 1.9)
CMIP6-EC-Earth3-Veg_r1i1p1f1 ()	10 (2.6 ... 1.0e+4)	1.1 (0.47 ... 1.8)	2.0 (0.00010 ... 14)	0.42 (-0.20 ... 0.99)
CMIP6-GISS-E2-1-G_r1i1p1f2 ()	2.9 (0.12 ... 1.0e+4)	0.43 (-1.1 ... 2.3)	3.2 (1.4 ... 21)	0.59 (0.18 ... 1.0)
CMIP6-HadGEM3-GC31-LL_r1i1p1f3 ()	1.0e+4 (15 ... 1.0e+4)	1.7 (0.92 ... 2.4)	4.5 (2.1 ... 23)	1.0 (0.59 ... 1.5)
CMIP6-HadGEM3-GC31-MM_r1i1p1f3 ()	1.0e+4 (11 ... 1.0e+4)	1.9 (1.0 ... 2.8)	3.3 (2.1 ... 6.9)	1.1 (0.52 ... 1.4)
CMIP6-INM-CM4-8_r1i1p1f1 ()	1.0e+4 (3.2 ... 1.0e+4)	1.7 (0.31 ... 2.8)	7.9 (3.3 ... 28)	1.6 (0.78 ... 2.1)
CMIP6-IPSL-CM6A-LR_r1i1p1f1 ()	13 (2.3 ... 1.0e+4)	0.90 (0.14 ... 1.8)	11 (0.00010 ... 2.5e+2)	1.5 (0.42 ... 1.9)
CMIP6-MPI-ESM1-2-HR_r1i1p1f1 ()	1.7e+2 (6.0 ... 1.0e+4)	1.3 (0.39 ... 2.1)	3.3 (2.0 ... 10)	0.96 (0.56 ... 1.4)

Table 2 (continued)

CMIP6-MRI-ESM2-0_r1i1p1f1 ()	3.6 (0.94 ... 58)	0.81 (-0.040 ... 1.6)	2.8 (0.00010 ... 6.1)	0.71 (0.13 ... 1.4)
CMIP6-NorESM2-LM_r1i1p1f1 ()	14 (2.2 ... 1.0e+4)	1.2 (0.46 ... 2.0)	3.7 (0.65 ... 16)	0.62 (0.020 ... 1.2)
CMIP6-NorESM2-MM_r1i1p1f1 ()	2.4 (0.45 ... 5.0e+3)	0.66 (-0.34 ... 1.6)	4.1 (0.00010 ... 36)	0.60 (0.030 ... 1.1)
CMIP6-TaiESM1_r1i1p1f1 ()	6.0 (1.5 ... 1.0e+4)	1.0 (0.18 ... 1.8)	6.4 (3.2 ... 29)	1.1 (0.84 ... 1.5)
CMIP6-UKESM1-0-LL_r1i1p1f2 ()	3.8 (2.1 ... 1.0e+3)	1.3 (0.77 ... 1.8)	2.8 (1.7 ... 11)	0.82 (0.52 ... 1.2)
CORDEX22-MPIr1-REMO ()	3.1 (0.35 ... 1.0e+4)	0.57 (-0.57 ... 1.6)	3.0 (1.5 ... 19)	0.82 (0.37 ... 1.3)
CORDEX22-MPIr1-REGCM ()	11 (1.5 ... 1.0e+4)	0.90 (0.0 ... 1.8)	9.1 (0.00010 ... 7.4e+2)	1.3 (0.97 ... 1.7)

Ciavarella et al. (2021), based on their performances in terms of the three criteria discussed above. Finally, if the model is 'good' for all of these criteria, we give it an overall rating of 'good' (green highlight in Table S1). We rate the model as 'reasonable' or 'bad', if it is rated 'reasonable' or 'bad', respectively, for at least one of the three criteria. These are respectively shown highlighted in yellow and red in Table S1. For the study area, 48 out of 72 considered models were used (Table 2), being those which were evaluated to be 'good' (the best estimate of the fit parameter for the models is within the confidence interval of the observed parameter estimate) or 'reasonable' (the confidence intervals of the model and observed parameters estimates overlap, but the best estimate of the models is outside the 95% confidence interval in the observations) (Ciavarella et al. 2021).

4.2 Multi-method multi-model attribution and hazard synthesis

For the event definition described above, we evaluated the influence of anthropogenic climate change on the event by calculating the PR as well as the change in intensity (ΔI) using observations and climate models. Taking into consideration the model evaluation shown in Table S1, we analysed the PRs and ΔI for the different models. Table 2 shows the model-based results for those models that are labeled 'reasonable' or 'good' in Table S1. The aim is to synthesise results from models that pass the evaluation along with the observations-based products, to give an overarching attribution statement. Figures 5 and 6 show the changes in probability and intensity for the observation-based products (blue) and models (red). To combine them into a synthesised assessment, a term to account for intermodel spread is added (in quadrature) to the natural variability of the models. This is shown in the figures as white boxes around the light red bars (in this study, only the intensity changes show intermodel spread beyond the models'
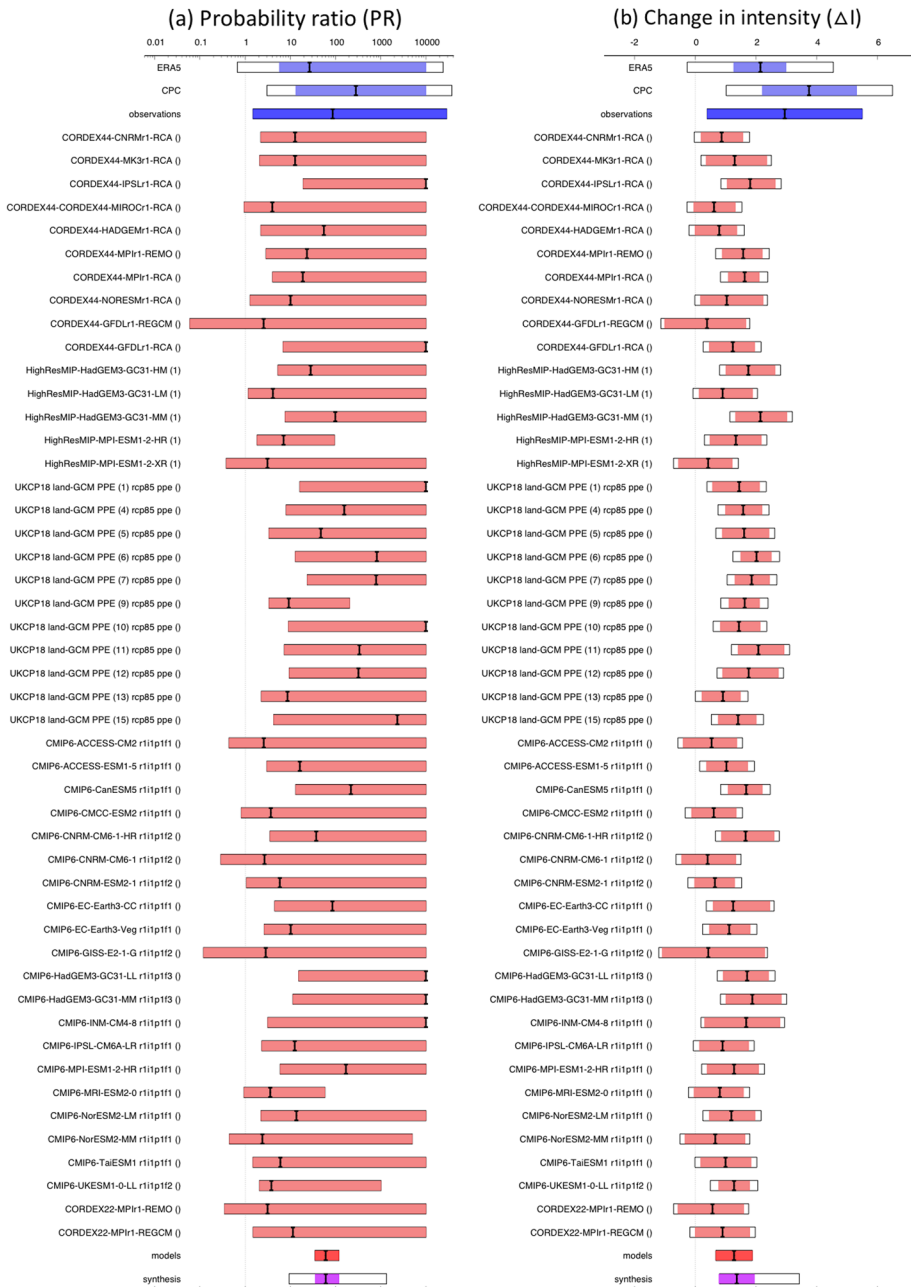
Fig. 5 Synthesis of (**a**) probability ratios and (**b**) intensity changes when comparing the return period and magnitudes of the 7-day average maximum temperatures over the study region in the current climate and a 1.2 °C cooler climate
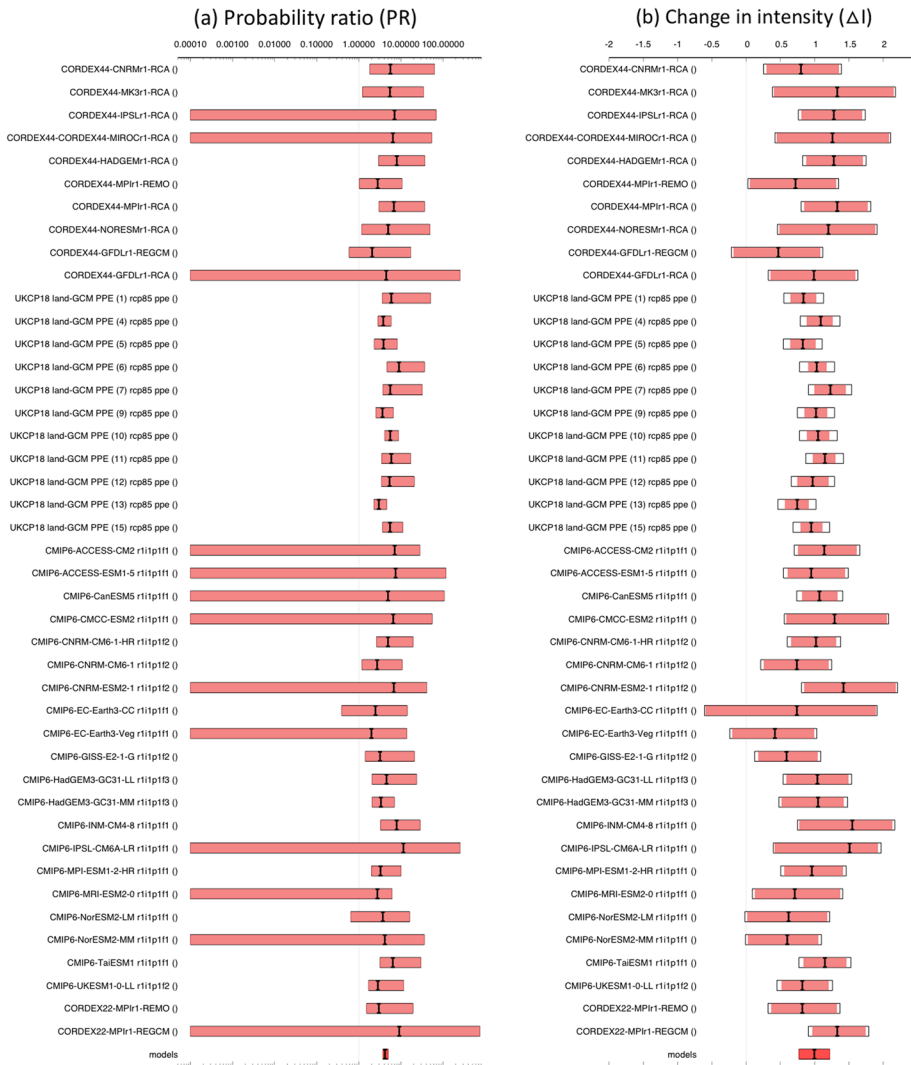
Fig. 6 As Fig. 5, but for models only of a 0.8 °C warmer (2 °C since pre-industrial) climate

natural variability). The dark red bar shows the model average, consisting of a weighted mean using the (uncorrelated) uncertainties due to natural variability plus the term representing intermodel spread (i.e., the inverse square of the white bars). Observation-based products and models are combined into a single result in two ways. Firstly, we neglect common model uncertainties beyond the intermodel spread that is depicted by the model average, and compute the weighted average of models (dark red bar) and observations (blue bar): this is indicated by the magenta bar. As, due to common model uncertainties, model uncertainty can be larger than the intermodel spread, secondly, we also show the more conservative estimate of an unweighted, direct average of observations (dark red bar) and models (dark blue bar) contributing 50% each, indicated by the white box around the magenta bar in Figs. 5 and 6.

For the PR, the best estimate of the models combined is well within the uncertainty of the observed change and the weighted synthesised PR is 60 [35–120]. Given however that the discrepancy between individual models with respect to the best guess is very large, spanning orders of magnitude and the quantification of changes in heat extremes is notoriously difficult, we report the best guess of a PR of 60 as our main result, but use the unweighted uncertainty to estimate the lower and upper bound: 9–1300. For the change in intensity we notice that the observed increase in intensity is larger than that of the models but again well within the uncertainty bounds. For the same reasons as above, we also report the unweighted bounds as our overarching result. The change in intensity attributable to human-induced climate change is 1.4 °C [0.8–3.4].

Looking at the simulations of potential further changes in a 0.8℃ warmer world compared with today we find that while some models have a lower bound below unity for the PR, all best estimates are greater than 1 and show, as expected in a warming world, a further increase of a factor of 4 in the likelihood of a heatwave like the observed to occur. This is an order of magnitude smaller than the thus far observed change in likelihood of a factor of approximately 60 which cannot be explained by the slightly smaller GMST change alone. Thus, without further analysis as to why these changes are so different, we do treat the quantitative estimate with caution. The change in intensity with a further 0.8℃ of warming is 1℃ (0.8–1.2) which is very much in line with the estimated changes in intensity that have occurred up to present and highlights again that, for heat waves, changes in intensity are much less sensitive to individual models and methods and thus the more reliable quantitative results to communicate.

5 Vulnerability, exposure and impacts

Heatwaves can highly affect society and the environment, with large impacts on human health, agriculture, the occurrence of wildfires, and infrastructure failures (Perkins-Kirkpatrick and Lewis 2020). The full impact of a heatwave on human health is often not known until weeks or months afterwards, once death certificates are collected, and data on excess deaths is analysed (Sahani et al. 2022). Impacts are an effect of pre-existing social, economic, political conditions which adds to vulnerability over the region. Data on excess deaths was not available at the time of writing, however it is notable that this heatwave occurred very early in the austral summer season. Early season heatwaves are known to be more deadly because people may not be prepared or acclimatized to high temperatures (Anderson and Bell 2011). A study comprising 326 Latin American cities, 26 of them located over our study area, found that marginal increases in hot temperatures results in a steep increase in mortality, with the strongest risks among older adults and for cardiovascular and respiratory deaths (Kephart et al. 2022). Typically, people with pre-existing health conditions, those that are over 65 or under five, have low incomes, work indoors with poor ventilation in homes or factories, and outdoor workers are more vulnerable to heat stress, heat stroke, or death (Green et al. 2019). In particular, previous studies considering some recent (2005–2015) heatwaves in Argentina, documented an increase in death risk for people over 60, particularly those older than 80, and individuals under 15 years of age (Chesini et al. 2019, 2022).

An early warning system for heatwaves have been developed in Argentina by the SMN and became operative during the summer of 2018 (Herrera et al. 2021). This system operates during the warm season (October to March) issuing daily alerts for 57 locations of

the country, with the aim of enabling both the population and civil protection agencies to take appropriate prevention, mitigation and response measures at each alert level (Chesini et al. 2022). If there is a heat risk alert (yellow, orange, or red) for the following 24 h, the Ministry of Security and the Ministry of Health are notified and the Ministry of Health will launch an epidemiological alert and make it public through social media, press agencies, and national media, with recommended actions to the general population and at-risk groups. For central and northern Argentina, the first heat warning was issued on December 2, two days prior to the start of the December heatwave. In the case of Paraguay, while the country lacks a heatwave early warning system, a special bulletin for persistent high temperatures was issued during December 7, while the same day Uruguayan authorities released a heatwave warning for the western portion of the country. Governments, city authorities and civil society organizations can prevent heat-related impacts by acting in anticipation of a forecast heatwave, after the issuance of an early warning and before the heatwave onset.

Cities are often hotspots of heat risk due to the urban heat island effect. With expanding urban land this effect will intensify in the future (Huang et al. 2019). Worth noting is that Argentina is amongst the most urbanized countries in the world, with 92 percent of people living in urban areas (Bolay 2020). In our study area, almost 45 million inhabitants were potentially affected by the heatwave conditions, most of them located in highly populated cities such as Buenos Aires and Asunción. In the Metropolitan Area of Asunción, over 400 informal settlements are home to 38.000 residents. Less than one percent of these inhabitants have access to sanitary sewages and 12 percent lack piped water, increasing their risk of contracting disease and reducing their coping capacity to extreme heat (Sandoval and Samiento 2020). In Argentina, approximately 1 in 10 people live in informal settlements, with the majority of informal settlements located in the city of Buenos Aires totaling roughly 300,000 people (Macció and Mitchell 2023; Palacios et al. 2022). Social cohesion can reduce heat-related mortality, but in informal settlements in Argentina, a lack of public spaces and recreational areas limits social cohesion and development (Yardley et al. 2011).

Recently, thermal resilience in building design was shown to provide indoor comfort to face heatwaves (Flores-Larsen et al. 2023), a factor that was considered in the modification of existing building codes for large cities such as Buenos Aires. This includes natural ventilation, envelope thermal insulation, green walls and roof (Flores-Larsen and Filippín 2021; Robbiati et al. 2022). While there are examples of heat-informed urban planning and adaptation outside of the capital (Fabián et al. 2021; Flores-Larsen and Filippín 2021), there would be notable benefits to their mainstreaming in other urban centers in heatwave-prone northern Argentina, some of which are up to twice as densely populated as Buenos Aires and home to a significant number of low-income populations (such as Rosario, Córdoba, Tucumán, and Corrientes). In contrast, Paraguay does not currently have an energy building code nor widespread use of other heat-related interventions, negatively affecting the population's coping capacity during heatwaves (Silvero et al. 2019). Energy shortcuts occurred in Buenos Aires city in response to a record high electricity demand in Argentina, affecting more than half million people due to the high energy demand (Infobae 2022). This highlights the vulnerability to heatwaves of the electricity distribution system of the metropolitan area of Buenos Aires, which has almost 7 times more probability of failure compared to cold events (Santágata et al. 2017).

Impacts related to heatwaves in Southern South America are not only restricted to society. For instance, in the last 40 years the number of fires and areas burned by wildfires have increased significantly, partly due to increases in temperature, threatening biodiversity (Jolly et al. 2015). In addition, several wildfires were reported over central-northern

Argentina by the time of occurrence of the analyzed heatwave, affecting up to 8 provinces (Ministerio de Ambiente y Desarrollo Sostenible 2022). In general, a more frequent occurrence of intense and long heatwaves has negative impacts in water and food systems, human health, terrestrial and freshwater ecosystems, among other systems that exhibit high or very high vulnerability in Southern South America (Castellanos et al. 2022).

6 Summary and discussion

During late November and early December 2022, a large area including the central-northern part of Argentina, southern Bolivia, central Chile, and most of Paraguay and Uruguay experienced record-breaking temperatures during two consecutive heatwaves. During early December, temperatures exceeded 40 °C in 24 locations, four of them above 45 °C. Rivadavia station, located near the border with Bolivia and Paraguay, recorded 46 °C of maximum temperature on December 7, making the region one of the hottest in the world during that day. During the heatwave, nine locations in northern Argentina registered their highest maximum temperature of December since at least 1961. Using published peer-reviewed methods based on different observational and reanalysis datasets, as well as global and regional model simulations, we analysed how human-induced climate change altered the likelihood and intensity of the 7-day heatwave event that occurred on 4–10 December 2022 in Southern South America.

Our analysis based on observational and reanalysis datasets indicate that South America, like the rest of the world, has experienced heatwaves increasingly frequently in recent years. The December 2022 heatwave, averaged over 7 days over the region shown in Fig. 1, has an estimated return time of 1 in 20 years in the current climate, meaning it has about a 5% chance of happening each year. We further looked at 7 individual weather stations to see whether the character of the heatwave differed within the study region. We found that at most stations the 7-day maximum temperatures observed during this heatwave have return times comparable to the region average -meaning it was equally unusual across much of the region- but the heat was more extreme towards the northwest of the region.

To estimate how human-caused climate change has influenced the likelihood and intensity of the observed heatwave, we combine climate models with the observations-based data. We found that human-caused climate change made the event about 60 times more likely. In this sense, a heatwave with a similar probability (return time of 1 in 20 years) would be about 1.4 °C less hot in a world that had not been warmed by human activities. With future global warming, heatwaves like this will become even more common and hotter. If global mean temperatures rise an additional 0.8 °C, to a total warming of 2 °C, a heatwave as hot as this one would have a return period of 5 instead of 20 years, while a heatwave that happens approximately once in 20 years would be 0.7–1.2 °C hotter than this one. It is important to highlight that there is a discrepancy between the modeled and observed change in heatwave intensity in the region, with the observations showing a larger increase. While there is no doubt that future heat extremes will become even hotter than they are now, this discrepancy limits confidence in projections of the magnitude of future extremes.

The 2022 heatwave led to large-scale power outages, wildfires and, in combination with the ongoing drought over the region, poor harvests. It is estimated to have led to an increase in heat-related deaths, with the impacts unequally distributed across demographics. In different cities and municipalities across South America, people living in some areas

-often marginal neighbourhoods- experience higher temperatures than others, as they lack green space, adequate thermal insulation from heat, electricity, shade, and water which can be lifelines during heatwaves.

Heatwaves this early in the summer season pose a substantial risk to human health and are potentially lethal. This risk is aggravated by climate change, but also by other factors such as an aging population, urbanisation and the built environment, and individual behavior and susceptibility to the heat. The full impact will only be known after several months or even years when the mortality figures have been analysed. Effective heat emergency plans, together with accurate weather forecasts such as those issued before this heatwave, reduce impacts and are becoming even more important in light of the rising risks. Heatwaves are a regular occurrence in Paraguay and Argentina and as the attribution analysis indicates, these types of events are increasing in frequency and intensity, which adds urgency to the need to adapt to this new normal. Investments in improving heat early warning systems, urban planning for heat, and behavioural change communication can help to reduce heat impacts now and in the future.

Data availability Almost all data is available via the KNMI Climate Explorer (https://climexp.knmi.nl/).

Declarations

Conflict of interest The authors declare they have no financial interests.

References

Alvarez MS, Cerne B, Osman M, Vera C (2019) Intraseasonal and low frequency processes contributing to the December 2013 heat wave in Southern South America. Clim Dyn 53:4977–4988. https://doi.org/10.1007/s00382-019-04838-6

Anderson GB, Bell ML (2011) Heat waves in the United States: mortality risk during heat waves and effect modification by heat wave characteristics in 43 U.S. communities. Environ Health Perspect 119(2):210–218. https://doi.org/10.1289/ehp.1002313

Barros VR, Boninsegna JA, Camilloni IA, Chidiak M, Magrín GO, Rusticucci M (2015) Climate change in Argentina: trends, projections, impacts and adaptation. Wires Clim Change 6:151–169. https://doi.org/10.1002/wcc.316

Bolay JC (2020) Urban Dynamics and Regional Development in Argentina. In: Bolay JC (ed) Urban Planning Against Poverty. Springer, Cham, Switzerland, pp 167–202. https://doi.org/10.1007/978-3-030-28419-0_6

Cabré F, Nuñez M (2020) Impacts of climate change on viticulture in Argentina. Reg Environ Change 20:12. https://doi.org/10.1007/s10113-020-01607-8

Cai W, McPhaden MJ, Grimm AM et al (2020) Climate impacts of the El Niño-Southern Oscillation on South America. Nat Rev Earth Environ 1:215–231. https://doi.org/10.1038/s43017-020-0040-3

Campetella C, Rusticucci M (1998) Synoptic analysis of an extreme heat wave over Argentina in March 1980. Meteorol Appl 5(3):217–226. https://doi.org/10.1017/S1350482798000851

Castellanos, E, Lemos MF, Astigarraga L et al (2022) Central and South America. In: Climate Change 2022: Impacts, Adaptation and Vulnerability. Contribution of Working Group II to the Sixth Assessment Report of the Intergovernmental Panel on Climate Change [Pörtner H-O, Roberts DC, Tignor M, Poloczanska ES, Mintenbeck K, Alegría A, Craig M, Langsdorf S, Löschke S, Möller V, Okem

A, Rama B (eds.)]. Cambridge University Press, Cambridge, UK and New York, NY, USA, pp 1689–1816. https://doi.org/10.1017/9781009325844.014

Ceccherini G, Russo S, Ameztoy I, Romero CP, Carmona-Moreno C (2016) Magnitude and frequency of heat and cold waves in recent decades: the case of South America. Nat Hazards Earth Syst Sci 16:821–831. https://doi.org/10.5194/nhess-16-821-2016

Cerne SB, Vera CS, Liebmann B (2007) The nature of a heat wave in Eastern Argentina occurring during SALLJEX. Mon Wea Rev 135(3):1165–1174. https://doi.org/10.1175/MWR3306.1

Chan D, Vecchi GA, Yang W, Huybers P (2021) Improved simulation of 19th- and 20th-century North Atlantic hurricane frequency after correcting historical sea surface temperatures. Sci Adv 7(26):eabg6931. https://doi.org/10.1126/sciadv.abg6931

Chesini F, Herrera N, Skansi MM, González-Morinigo C, Fontán S, Savoy F, de Titto E (2022) Mortality risk during heat waves in the summer 2013–2014 in 18 provinces of Argentina: Ecological study. Ciênc Saúde Coletiva 27(5):2071–2086. https://doi.org/10.1590/1413-81232022275.07502021

Chesini F, Abrutzky R, de Titto EH (2019) Mortalidad por olas de calor en la Ciudad de Buenos Aires, Argentina (2005–2015). Cad Saude Publica 35(9):e00165218. https://doi.org/10.1590/0102-311X00165218

Ciavarella A, Cotterill D, Stott P et al (2021) Prolonged Siberian heat of 2020 almost impossible without human influence. Clim Change 166:9. https://doi.org/10.1007/s10584-021-03052-w

Delworth TL, Rosati A, Anderson W, Adcroft AJ, Balaji V, Benson R, Dixon K, Griffies SM, Lee H, Pacanowski RC, Vecchi GA, Wittenberg AT, Zeng F, Zhang R (2012) Simulated climate and climate change in the GFDL CM2.5 High-Resolution Coupled Climate Model. J Clim 25(8):2755–2781. https://doi.org/10.1175/JCLI-D-11-00316.1

DMH (2022) Boletín Meteorológico Especial. https://www.meteorologia.gov.py/wp-content/uploads/2022/12/202212070920_altas_-temperaturas.pdf. Accessed 16 February 2023

Eyring V, Bony S, Meehl GA, Senior CA, Stevens B, Stouffer RJ, Taylor KE (2016) Overview of the Coupled Model Intercomparison Project Phase 6 (CMIP6) experimental design and organization. Geosci Model Dev 9:1937–1958. https://doi.org/10.5194/gmd-9-1937-2016

Fabian D, González E, Sánchez MV, Salvo A, Fenoglio MS (2021) Towards the design of biodiverse green roofs in Argentina: assessing key elements for different functional groups of arthropods. Urban For Urban Green 61:127107. https://doi.org/10.1016/j.ufug.2021.127107

Falco M, Carril AF, Menéndez CG, Zaninelli PG, Li LZX (2019) Assessment of CORDEX simulations over South America: added value on seasonal climatology and resolution considerations. Clim Dyn 52:4771–4786. https://doi.org/10.1007/s00382-018-4412-z

Feron S, Cordero RR, Damiani A et al (2019) Observations and Projections of Heat Waves in South America. Sci Rep 9:8173. https://doi.org/10.1038/s41598-019-44614-4

Flores-Larsen S, Filippín C, Bre F (2023) New metrics for thermal resilience of passive buildings during heat events. Build Environ 230:109990. https://doi.org/10.1016/j.buildenv.2023.109990

Flores-Larsen S, Filippín C (2021) Energy efficiency, thermal resilience, and health during extreme heat events in low-income housing in Argentina. Energy Build 231:110576. https://doi.org/10.1016/j.enbuild.2020.110576

Geirinhas JL, Trigo RM, Libonati R, Coelho CAS, Palmeira AC (2018) Climatic and synoptic characterization of heat waves in Brazil. Int J Climatol 38:1760–1776. https://doi.org/10.1002/joc.5294

Green H, Bailey J, Schwarz L, Vanos J, Ebi K, Benmarhnia T (2019) Impact of heat on mortality and morbidity in low and middle income countries: A review of the epidemiological evidence and considerations for future research. Environ Res 171:80–91. https://doi.org/10.1016/j.envres.2019.01.010

Gutowski WJ Jr, Giorgi F, Timbal B, Frigon A, Jacob D, Kang H-S, Raghavan K, Lee B, Lennard C, Nikulin G, O'Rourke E, Rixen M, Solman S, Stephenson T, Tangang F (2016) WCRP COordinated Regional Downscaling EXperiment (CORDEX): a diagnostic MIP for CMIP6. Geosci Model Dev 9:4087–4095. https://doi.org/10.5194/gmd-9-4087-2016

Haarsma RJ, Roberts MJ, Vidale PL et al (2016) High Resolution Model Intercomparison Project (HighResMIP v1.0) for CMIP6. Geosci Model Dev 9:4185–4208. https://doi.org/10.5194/gmd-9-4185-2016

Hannart A, Vera C, Cerne B, Otto FEL (2015) Causal Influence of Anthropogenic Forcings on the Argentinian Heat Wave of December 2013. Bull Am Meteor Soc 96(12):S41–S45. https://doi.org/10.1175/BAMS-D-15-00137.1

Hansen J, Ruedy R, Sato M, Lo K (2010) Global surface temperature change. Rev Geophys 48:RG4004. https://doi.org/10.1029/2010RG000345

Herrera N, Chesini F, Saucedo MA, Menalled ME, Fernández C, Chasco J, Cejas AG (2021) Sistema de Alerta Temprana por Temperaturas Extremas Calor (SAT-TE Calor): la evolución del SAT-OCS. Technical Note SMN 2021–111. http://repositorio.smn.gob.ar/handle/20.500.12160/1726. Accessed 22 June 2023

Hersbach H, Bell B, Berrisford P et al (2020) The ERA5 global reanalysis. Q J R Meteorol Soc 146:1999–2049. https://doi.org/10.1002/qj.3803

Huang K, Li X, Liu X, Seto KC (2019) Projecting global urban land expansion and heat island intensification through 2050. Environ Res Lett 14(11):114037. https://doi.org/10.1088/1748-9326/ab4b71

Infobae (2022) El Gobierno sancionará a Edenor y Edesur por dejar hasta 570.000 usuarios sin servicio eléctrico a lo largo del fin de semana. https://www.infobae.com/economia/2022/12/11/tormenta-calor-y-cortes-de-luz-el-gobierno-sancionara-a-edenor-y-edesur-por-dejar-hasta-570000-usuarios-sin-electricidad-a-lo-largo-del-fin-de-semana/. Accessed 23 March 2023

INUMET (2022a) Boletín Climático Noviembre 2022a. https://www.inumet.gub.uy/sites/default/files/2022a-12/BOLETIN/20CLIMÁTICO/20NOVIEMBRE/202022a.pdf. Accessed 16 February 2023

INUMET (2022b) Departamento de Pronóstico del Tiempo y Vigilancia Meteorológica: Aviso Meteorológico Vigente. https://www.inumet.gub.uy/reportes/riesgo/pdf/adv1670418154527.pdf. Accessed 16 February 2023

IPCC (2021) Summary for Policymakers. In: Climate Change 2021: The Physical Science Basis. Contribution of Working Group I to the Sixth Assessment Report of the Intergovernmental Panel on Climate Change [Masson-Delmotte V, Zhai P, Pirani A, Connors SL, Péan C, Berger S, Caud N, Chen Y, Goldfarb L, Gomis MI, Huang M, Leitzell K, Lonnoy E, Matthews JBR, Maycock TK, Waterfield T, Yelekçi O, Yu R, and Zhou B (eds.)]. Cambridge University Press, Cambridge, United Kingdom and New York, NY, USA, pp 3–32. https://doi.org/10.1017/9781009157896.001

Jolly W, Cochrane M, Freeborn P et al (2015) Climate-induced variations in global wildfire danger from 1979 to 2013. Nat Commun 6:7537. https://doi.org/10.1038/ncomms8537

Kephart JL, Sánchez BN, Moore J et al (2022) City-level impact of extreme temperatures and mortality in Latin America. Nat Med 28:1700–1705. https://doi.org/10.1038/s41591-022-01872-6

Lenssen NJL, Schmidt GA, Hansen JE, Menne MJ, Persin A, Ruedy R, Zyss D (2019) Improvements in the GISTEMP uncertainty model. J Geophys Res: Atmos 124:6307–6326. https://doi.org/10.1029/2018JD029522

Lowe JA, Bernie D, Bett P, Bricheno L et al (2018) UKCP18 Science Overview Report. Met Office, London

Macció J, Mitchell A (2023) Medición multidimensional de Pobreza en ciudades segregadas evidencia de la ciudad de Buenos Aires. Rev Desarro Soc 93:101–137. https://doi.org/10.13043/DYS.93.3

Marengo JA, Ambrizzi T, Barreto N, Cunha AP, Ramos AM, Skansi M, Molina Carpio J, Salinas R (2022) The heat wave of October 2020 in central South America. Int J Climatol 42(4):2281–2298. https://doi.org/10.1002/joc.7365

Ministerio de Ambiente y Desarrollo Sostenible (2022) Manejo del fuego - Reporte de incendios correspondiente al 6 de diciembre de 2022. https://www.argentina.gob.ar/sites/default/files/2022/12/reporte_6_diciembre.pdf. Accessed 23 March 2023

Naumann G, Podestá G, Marengo J et al (2023) Extreme and long-term drought in the La Plata Basin: event evolution and impact assessment until September 2022. Publications Office of the European Union, Luxembourg. https://doi.org/10.2760/62557

Otto F, Skeie R, Fuglestvedt J et al (2017) Assigning historic responsibility for extreme weather events. Nature Clim Change 7:757–759. https://doi.org/10.1038/nclimate3419

Palacios A, Gabosi J, Williams CR, Rojas-Roque C (2022) Social vulnerability, exposure to environmental risk factors, and accessibility of healthcare services: Evidence from 2,000+ informal settlements in Argentina. Soc Sci Med 309:115290. https://doi.org/10.1016/j.socscimed.2022.115290

Perkins-Kirkpatrick SE, Lewis SC (2020) Increasing trends in regional heatwaves. Nat Commun 11:3357. https://doi.org/10.1038/s41467-020-16970-7

Philip S, Kew S, van Oldenborgh GJ et al (2020) A protocol for probabilistic extreme event attribution analyses. Adv Stat Clim Meteorol Oceanogr 6:177–203. https://doi.org/10.5194/ascmo-6-177-2020

Ranasinghe R, Ruane AC, Vautard R, Arnell N, Coppola E et al (2021) Climate Change information for regional impact and for risk assessment. In Climate Change 2021: The physical science basis. Contribution of Working group i to the sixth assessment report of the intergovernmental panel on climate change [Masson-Delmotte V, Zhai P, Pirani A, Connors SL, Péan C, Berger S, Caud N, Chen Y, Goldfarb L, Gomis MI, Huang M, Leitzell K, Lonnoy E, Matthews JBR, Maycock TK, Waterfield T, Yelekçi O, Yu R, and Zhou B (eds.)]. Cambridge University Press, Cambridge, United Kingdom and New York, NY, USA, pp 1767–1926. https://doi.org/10.1017/9781009157896.014

Rayner NA, Parker DE, Horton EB, Folland CK, Alexander LV, Rowell DP, Kent EC, Kaplan A (2003) Global analyses of sea surface temperature, sea ice, and night marine air temperature since the late nineteenth century. J Geophys Res 108:4407. https://doi.org/10.1029/2002JD002670

Reboita MS, Kuki CAC, Marrafon VH et al (2022) South America climate change revealed through climate indices projected by GCMs and Eta-RCM ensembles. Clim Dyn 58:459–485. https://doi.org/10.1007/s00382-021-05918-2

Robbiati FO, Cáceres N, Hick EC, Suarez M, Soto S, Barea G, Matoff E, Galetto L, Imhof L (2022) Vegetative and thermal performance of an extensive vegetated roof located in the urban heat island of a semiarid region. Build Environ 212:108791. https://doi.org/10.1016/j.buildenv.2022.108791

Rusticucci M, Kysely J, Almeira G, Lhotka O (2016) Long-term variability of heat waves in Argentina and recurrence probability of the severe 2008 heat wave in Buenos Aires. Theor Appl Climatol 124:679–689. https://doi.org/10.1007/s00704-015-1445-7

Sahani J, Kumar P, Debele S, Emmanuel R (2022) Heat risk of mortality in two different regions of the United Kingdom. Sustain Cities Soc 80:103758. https://doi.org/10.1016/j.scs.2022.103758

Sandoval V, Sarmiento JP (2020) A neglected issue: informal settlements, urban development, and disaster risk reduction in Latin America and the Caribbean. Disaster Prev Manag 29(5):731–745. https://doi.org/10.1108/DPM-04-2020-0115

Santagata DM, Castesana P, Rossler CE, Gómez DR (2017) Extreme temperature events affecting the electricity distribution system of the metropolitan area of Buenos Aires (1971–2013). Energy Policy 106:404–413. https://doi.org/10.1016/j.enpol.2017.04.006

Seneviratne SI, Zhang X, Adnan M, Badi W, Dereczynski C et al (2021) Weather and climate extreme events in a changing climate. In Climate Change 2021: The physical science basis. contribution of working group I to the sixth assessment report of the intergovernmental panel on climate change [Masson-Delmotte V, Zhai P, Pirani A, Connors SL, Péan C, Berger S, Caud N, Chen Y, Goldfarb L, Gomis MI, Huang M, Leitzell K, Lonnoy E, Matthews JBR, Maycock TK, Waterfield T, Yelekçi O, Yu R, and Zhou B (eds.)]. Cambridge University Press, Cambridge, United Kingdom and New York, NY, USA, pp 1513–1766. https://doi.org/10.1017/9781009157896.013

Silvero F, Lops C, Montelpare S et al (2019) Impact assessment of climate change on buildings in Paraguay—Overheating risk under different future climate scenarios. Build Simul 12:943–960. https://doi.org/10.1007/s12273-019-0532-6

SMN (2023) Informe Especial N°8 por ola de calor / altas temperaturas temporada 2022–2023. https://www.smn.gob.ar/sites/default/files/informe_oladecalor_2-15febrero2023.pdf. Accessed 16 February 2023

SMN (2022a) Informe Especial N°2 por ola de calor / altas temperaturas temporada 2022a-2023. https://www.smn.gob.ar/sites/default/files/informe_oladecalor_23-29noviembre2022a.pdf. Accessed 16 February 2023

SMN (2022b) Boletín Climatológico Noviembre 2022b. https://www.smn.gob.ar/sites/default/files/ClimNov2022b.pdf. Accessed 16 February 2023

SMN (2022c) Informe Especial N°3 por ola de calor / altas temperaturas temporada 2022c-2023. https://www.smn.gob.ar/sites/default/files/informe_oladecalor_4-12diciembre2022c.pdf. Accessed 16 February 2023

Taylor KE, Stouffer RJ, Meehl GA (2012) An overview of CMIP5 and the experiment design. Bull Am Meteor Soc 93(4):485–498. https://doi.org/10.1175/BAMS-D-11-00094.1

van Garderen L, Mindlin J (2022) A storyline attribution of the 2011/2012 drought in Southeastern South America. Weather 77(6):212–218. https://doi.org/10.1002/wea.4185

van Oldenborgh GJ, van der Wiel K, Kew S et al (2021) Pathways and pitfalls in extreme event attribution. Clim Change 166(1):13. https://doi.org/10.1007/s10584-021-03071-7

Vecchi GA, Delworth T, Gudgel R et al (2014) On the seasonal forecasting of regional tropical cyclone activity. J Clim 27(21):7994–8016. https://doi.org/10.1175/JCLI-D-14-00158.1

Yang W, Hsieh T-L, Vecchi GA (2021) Hurricane annual cycle controlled by both seeds and genesis probability. PNAS 118(41):e2108397118. https://doi.org/10.1073/pnas.2108397118

Yardley J, Sigal RJ, Kenny GP (2011) Heat health planning: The importance of social and community factors. Glob Environ Chang 21(2):670–679. https://doi.org/10.1016/j.gloenvcha.2010.11.010

Authors and Affiliations

Juan Antonio Rivera[1] [ORCID] **· Paola A. Arias[2] · Anna A. Sörensson[3,4,5] · Mariam Zachariah[6] · Clair Barnes[6] · Sjoukje Philip[7] · Sarah Kew[7] · Robert Vautard[8] · Gerbrand Koren[9] · Izidine Pinto[7] · Maja Vahlberg[10] · Roop Singh[10] · Emmanuel Raju[11] · Sihan Li[12] · Wenchang Yang[13] · Gabriel A. Vecchi[13,14] · Luke J. Harrington[15] · Friederike E. L. Otto[6]**

✉ Juan Antonio Rivera
   jrivera@mendoza-conicet.gob.ar

[1] Instituto Argentino de Nivología, Glaciología Y Ciencias Ambientales (IANIGLA), CCT CONICET, Mendoza, Argentina

[2] Grupo de Ingeniería Y Gestión Ambiental (GIGA), Escuela Ambiental, Facultad de Ingeniería, Universidad de Antioquia, Medellín, Colombia

[3] Facultad de Ciencias Exactas Y Naturales, Universidad de Buenos Aires, Buenos Aires, Argentina

[4] Centro de Investigaciones del Mar Y La Atmósfera, CONICET–Universidad de Buenos Aires, Buenos Aires, Argentina

[5] CNRS–IRD–CONICET–UBA, Instituto Franco-Argentino Para El Estudio del Clima Y Sus Impactos (IRL 3351 IFAECI), Buenos Aires, Argentina

[6] Grantham Institute, Imperial College London, London, UK

[7] Royal Netherlands Meteorological Institute (KNMI), De Bilt, The Netherlands

[8] Institut Pierre-Simon Laplace, Paris, France

[9] Copernicus Institute of Sustainable Development, Utrecht University, Utrecht, The Netherlands

[10] Red Cross Red Crescent Climate Centre, The Hague, The Netherlands

[11] Department of Public Health, Global Health Section & Copenhagen Centre for Disaster Research, Copenhagen, Denmark

[12] Department of Geography, University of Sheffield, Sheffield, UK

[13] Department of Geosciences, Princeton University, Princeton, NJ 08544, USA

[14] High Meadows Environmental Institute, Princeton University, Princeton, NJ 08544, USA

[15] Te Aka Mātuatua School of Science, University of Waikato, Hillcrest, Hamilton 3214, New Zealand